Mon. Not. R. astr. Soc. (1991) **248,** 653–663

Dynamics of colliding binary stellar winds – pressure equilibrium models

Josef Kallrath
Astronomische Institut der Universität Bonn, Auf dem Hügel 71, 5300 Bonn 1, Germany

Accepted 1990 September 14. Received 1990 September 11; in original form 1990 April 18

SUMMARY

The dynamical and geometrical aspects of two quasi-radial supersonic counter-streaming gas flows are investigated in the framework of pressure equilibrium models. The numerical results, i.e. the boundary layers derived from the Newtonian approximation (orthogonal momentum conservation) and extended models based on mass and momentum conservation using constant velocity fields and fields with quadratically decreasing acceleration for a hot model (Wolf–Rayet/O-star) binary are compared with analytical approximations of the interface defined as an envelope derived from trajectorial models (two-fixed-centre problem, restricted three-body problem). The numerical integration yields a boundary curve which might be approximated by a hyperboloid. The envelope and the interface corresponding to given fields with quadratically decreasing acceleration fit nearly identically to each other. The results can serve as input data for an analysis of the binary stellar wind problems based on a shock-capturing method.

1 INTRODUCTION

The intention of this work and some related investigations (Kallrath 1989, 1990) is to contribute to the understanding of the complex physics in the boundary-layer region between two colliding quasi-radially symmetric supersonic flow fields occurring in hot binary star systems in the form of radiatively driven stellar winds.

A special case of interest arises if there are two stellar winds in hot (WR + O – star) binary systems as for example V444 Cygni, γ^2Vel or HD 152270: one has to model colliding supersonic flows with Mach numbers of about 100, leading to shock and contact surfaces. Such systems are of broad interest since many Wolf–Rayet stars are members of binary systems (30 per cent according to Moffat *et al.* 1986), and some motivation for a detailed and systematic discussion of the boundary layer between two colliding stellar wind flows has already been given by Kallrath (1989, 1990): this is referred to as the binary stellar wind problem (BSWP).

Usually, in the literature, one finds contributions on the dynamics of colliding binary stellar winds, or interaction of the solar wind and interstellar medium, which are related to the Newtonian-approximation (NA) based on conservation of orthogonal momentum (Fahr, Grezdzielski & Ratkiewicz-Landowska 1986b) or an extended models (Giuliani 1982) taking into account the conservation of mass and total momentum. Most of the analyses in the past, e.g. Huang & Weigert (1982) or Girard & Willson (1987), have been based on constant velocity fields (CVF), and assume the boundary layer to be of zero thickness, i.e. the shock fronts are identical with the contact surface. Shore & Brown (1988) have a model with constant velocity for the WR-star and a distance-dependent velocity of the O-star, although this velocity field does not imply a quadratically decreasing acceleration (QDA). Thus the goals of this paper and a subsequent one are as follows.

First, we derive boundary layers in the NA, then, based on the conservation of mass and momentum with external fields, discuss flows with QDA. These interfaces, and the external fields also, will be used in a forthcoming paper as input data for a shock-capturing method yielding the location and geometry of the boundary and the shock fronts.

Secondly, we compare the boundaries from these pressure-equilibrium models with the results derived by Kallrath (1989, 1990) where the boundary or separatrix between the two wind flows has been defined as the envelope of all iso-energetic trajectories originating on an equipotential surface of the Wolf–Rayet component.

By investigating the BSWP in the framework of the restricted three-body problem, the effect of non-inertial forces has been estimated by Kallrath (1989, 1990). For a model (WR/O) binary like HD 152270, this effect can be neglected to first order and justifies further analyses based on cylindrical symmetry.

Thirdly, we compare the results of the gas dynamical calculation to obtain information about the goodness of such pressure-equilibrium surfaces. In particular we test the assumption that the interface is of zero thickness. It will turn out in a forthcoming paper that this assumption is not entirely valid.

This paper is structured as follows. In Section 2.1, pressure-equilibrium surfaces (Fahr, Ratkiewicz-Landowska & Grezdzielski 1986a) are derived from the NA. The contact surface is determined by the requirement that the projections of the stress tensors on the surface normal or the orthogonal momentum flux on both sides of the (unknown) surface cancel each other. Furthermore, it is assumed that the interface between both wind flows is of zero thickness. In the case of axial symmetry, the surface can be calculated by an ordinary first-order differential equation (ODE). This ODE depends on given density and velocity fields. In Sections 2.1.1 and 2.1.2 we set up the nomenclature for CVFs and fields with QDA. Such models are often used as a simple model to describe the stellar wind of a single star, e.g. Castor, Abbott & Klein (1975) or Neutsch (1979).

A more refined model (Section 2.2), accounting for mass conservation and conservation of both orthogonal and parallel momentum flux, leads to a system of three coupled ODEs which we integrate by Bulirsch–Stoer extrapolation (Bulirsch & Stoer 1965). The input data to this procedure are given density- and velocity-fields in the region associated with either the WR- or O-star. In particular, the integrations are performed for CVFs and for models with isotropic QDA for a hot model (WR/O) binary with a set of parameters used by Neutsch (1979, 1986) to model HD 152270.

In Section 3 we summarize, compare and evaluate the results of the trajectorial model and those derived in this paper.

In a forthcoming paper the binary stellar wind problem is discussed in terms of a numerical integration of the hyperbolic system of partial differential equations describing the conservation of mass, momentum and energy, which govern the stellar wind fluid dynamics.

2.1 The Newtonian approximation

Let us consider two radial flow fields, i.e. velocity-, density- and pressure-fields with origins at $r_{\times 1}=(-a,0,0)^t$ and $r_{\times 2}=(+a,0,0)^t$ Star '1' is the Wolf–Rayet star and star '2' the O-star. The form of the velocity field is taken as given.

The boundary surface or the thin-shell interface should be determined as in Friend & Abbott (1986), i.e. by application of the NA. Thus, external to the interface the flow fields are the undisturbed fields of stellar winds emitted by single stars. For hypersonic flows this approximation seems to be justified. Within the NA, the interface $\mathbb{F}$ itself is assumed to be of zero thickness. This assumption, or even the weaker requirement that the interface will be thin, is only valid if the thermal energy of the shocked gas can be radiated away fast enough. This problem will be discussed in a later paper. The basic equation of the NA (Fahr *et al.* 1986a) is

$$\mathbf{\Pi}_{ik}n_in_k|_1=\mathbf{\Pi}_{ik}n_in_k|_2, \tag{2.1}$$

where $\mathbf{\Pi}_{ik}$ is the pressure tensor and n_i, n_k are the components of the normal vector $\boldsymbol{n}$ at a point of $\mathbb{F}$. If no magnetic fields are present, $\mathbf{\Pi}_{ik}$ is

$$\mathbf{\Pi}_{ik}:=p\delta_{ik}+\rho v_iv_k. \tag{2.2}$$

Equation (2.1) describes the equality of the normal components of the hydrodynamic momentum flux, i.e. the sum of the kinetic and thermal pressure, on both sides of the interface $\mathbb{F}$ defined by (2.1). From (2.1) and (2.2) it follows that

$$\rho v_n^2+p|_1=\rho v_n^2+p|_2, \tag{2.3}$$

where $v_n:=\boldsymbol{v}^t\cdot\boldsymbol{n}$ is the normal component of the velocity projected on to $\mathbb{F}$.

Since below we will concentrate only on radially symmetric density and velocity fields, let us furthermore make the assumptions curl $(\rho_i\boldsymbol{v}_i)=0$ and $\mathrm{div}(\rho_i\boldsymbol{v}_i)=-C_i\delta(\boldsymbol{r}_{\times i})$ for the single fields, where C_i is proportional to the mass-loss rate A_i. Under these assumptions, which are only valid for single radially symmetric fields, and $\rho_i\boldsymbol{v}_i=\nabla_\varphi$, from the Poisson equation $\Delta\varphi=-C_i\delta(\boldsymbol{r}_{\times i})$ we derive the solution

$$\rho_i\boldsymbol{v}_i=C_i(\boldsymbol{r}-\boldsymbol{r}_{\times i})\,r_i^{-3},\ C_i:=A_i/4\pi,\ r_i:=|\boldsymbol{r}-\boldsymbol{r}_{\times i}|, \tag{2.4}$$

where r_i denotes the distance to the stars. Eliminating $\boldsymbol{v}$ or v_n from (2.3) leads to an equation for $\mathbb{F}$ depending only on density and pressure fields

$$p_1+\frac{C_1^2}{\rho_1}\left|\frac{(\boldsymbol{r}-\boldsymbol{r}_{\times 1})\cdot\boldsymbol{n}}{r_1^3}\right|^2=\frac{C_2^2}{\rho_2}\left|\frac{(\boldsymbol{r}-\boldsymbol{r}_{\times 2})\cdot\boldsymbol{n}}{r_2^3}\right|^2+p_2. \tag{2.5}$$

Actually, the interface $\mathbb{F}$ is only a part of the set of all points $\boldsymbol{r}$ solving (2.5), since only the absolute values of $\boldsymbol{v}$ have been considered when deriving this equation. Thus, in addition to (2.5), we require

$$v_{1n}\cdot v_{2n}<0. \tag{2.6}$$

While Fahr *et al.* (1986a) use spherical coordinates to model the heliopause, and Huang & Weigert (1982) use Cartesian coordinates to investigate the colliding flows in a binary star system, we prefer cylindrical coordinates (from now on we use ρ as the polar coordinate which should not be confused with the mass densities ρ_1, ρ_2 and ρ_i which are always referred to with a subscript)

$$(x\in\mathbb{R},\ y=\rho\cos\varphi,\ z=\rho\sin\varphi), \tag{2.7}$$

where $\rho^2=y^2+z^2$ and $\tan\varphi=z/y$. These coordinates will reduce the partial differential equation (2.5) to an ordinary differential equation. For later use we note the following formulae and abbreviations:

$$\boldsymbol{r}-\boldsymbol{r}_{\times i}=[x-(-1)^ia,\ \rho\cos\varphi,\ \rho\sin\varphi]; \tag{2.8}$$

$$r_i=|\boldsymbol{r}-\boldsymbol{r}_{\times i}|=\sqrt{[x-(-1)^ia]^2+\rho^2}; \tag{2.9}$$

$$u:=u(x,a)=x+a,\quad v:=v(x,a)=x-a; \tag{2.10}$$

$$U:=U(\rho,x)=(x+a)^2+\rho^2=u^2+\rho^2; \tag{2.11}$$

$$V:=V(\rho,x)=(x-a)^2+\rho^2=v^2+\rho^2. \tag{2.12}$$

Now the normal vector $\boldsymbol{n}$ is a function of ρ, φ and x. The interface $\mathbb{F}$ may be parameterized by

$$\boldsymbol{r}_{\mathrm{G}}(\rho,\varphi)=[x(\rho,\varphi),\ \rho\cos\varphi,\ \rho\sin\varphi]. \tag{2.13}$$

Then, the normal vector $\boldsymbol{n}_{\mathrm{G}}(x,y,z)$ is given by the normalized cross-product

$$\boldsymbol{n}_{\mathrm{G}}(\rho,\varphi)=\boldsymbol{r}_{\mathrm{G},\rho}\times\boldsymbol{r}_{\mathrm{G},\varphi}/|\boldsymbol{r}_{\mathrm{G},\rho}\times\boldsymbol{r}_{\mathrm{G},\varphi}|. \tag{2.14}$$

Utilizing the azimuthal symmetry along the x-axis, i.e.

$$\boldsymbol{r}_{\mathrm{G}}(\rho,\varphi)=\boldsymbol{r}_{\mathrm{G}}(\rho),\ x_\varphi\equiv 0, \tag{2.15}$$

we finally achieve

$$\boldsymbol{n}:=\boldsymbol{n}_{\mathrm{G}}(\rho,\varphi)=[1,\ -x_\rho\cos\varphi,\ -x_\rho\sin\varphi]/[1+x_\rho^2]^{1/2}, \tag{2.16}$$

leading to

$$(\boldsymbol{r}-\boldsymbol{r}_i)\cdot\boldsymbol{n}=[x-(-1)^i a-\rho x_\rho]/[1+x_\rho^2]^{1/2}, \quad (2.17)$$

and

$$\mathrm{sign}[v_{1n}\cdot v_{2n}]=\mathrm{sign}[(x+a-\rho x_\rho)\cdot(x-a-\rho x_\rho)]. \quad (2.18)$$

Now we require a specification of ρ_i and p_i in (2.5) leading to a non-linear ordinary differential equation of first order in which we replace $x_\rho := \partial x/\partial\rho$ by $x' := dx/d\rho$ for easier reading.

With given radial-symmetric density- and pressure-fields $\rho_i := \rho_i(r_i)$ and $p_i := p_i(r_i)$ and some auxiliary functions

$$a_i := C_i^2/\rho_i r_i^6, \quad (2.19)$$

(2.5) is transformed to

$$p_1+a_1(u-\rho x')^2/(1+x'^2)=p_2+a_2(v-\rho x')^2/(1+x'^2). \quad (2.20)$$

If we further define

$$A := A[\rho, x(\rho)]=(p_1-p_2)+\rho^2(a_1-a_2), \quad (2.21)$$

$$B := B[\rho, x(\rho)]=\rho(a_1 u-a_2 v), \quad (2.22)$$

$$C := C[\rho, x(\rho)]=(p_1-p_2)+a_1 u^2-a_2 v^2, \quad (2.23)$$

and note that $1+x'^2 \geq 1$, our differential equation for $x(\rho)$ now reads

$$Ax'^2-2Bx'+C=0, \quad (2.24)$$

which can be treated as an initial value problem where we derive the initial value from the stagnation point $x_0 := x(\rho=0)$ according to the symmetry condition

$$x'_0 := x'(\rho=0)=0. \quad (2.25)$$

From (2.24 and 2.25) we calculate the stagnation point in the field of stars with radii R_1 and R_2 according to

$$C(0, x_0)=0, \ -a+R_2 \leq x_0 \leq a-R_1. \quad (2.26)$$

(2.26) is a sufficient condition which guarantees that not only is $C(0, x_0)=0$ fulfilled, but also that x_0 is not in the interior of one of the stars. In order to perform the integration let us transform (2.24) to

$$x'_{1,2}=\frac{B}{A}+\frac{k}{A}(B^2-CA)^{1/2}, \quad (2.27)$$

where $k=+1$ or $k=-1$ has to be chosen such that (2.6) is fulfilled also taking into account (2.18). For the numerical integration we used the extrapolation method by Bulirsch & Stoer (1965).

We will confine ourselves to the case that the thermal pressures p_i are negligible when compared with the kinetic pressures $\rho_i v_i^2$, i.e. we set $p_i=0$. This assumption, however, is not allowed if it leads to a scenario in which no stagnation point would formally exist between the stars. In that case, one would also have to take into account the fact that, from the stars' photospheres up to some critical surfaces, the winds move with subsonic speeds leading to a completely different physics.

The functions A, B and C in (2.21–2.23) take the form

$$A := A[\rho, x(\rho)]=\rho^2(a_1-a_2), \qquad A_0 := A(\rho=0)=0, \quad (2.28)$$

$$B := B[\rho, x(\rho)]=\rho(a_1 u-a_2 v), \qquad B_0 := B(\rho=0)=0, \quad (2.29)$$

$$C := C[\rho, x(\rho)]=a_1 u^2-a_2 v^2. \quad (2.30)$$

The differential equation (2.24) for $x(\rho)$ now takes the simplified form

$$x'_{1,2}=\frac{1}{\rho}\,\frac{a_1 u-a_2 v+2ka[a_1 a_2]^{1/2}}{a_1-a_2}, \quad k=\pm 1. \quad (2.31)$$

The general formalism will be applied to two important type of fields, namely those describing constant velocity fields (CVF) and fields with quadratically decreasing acceleration (QDA).

2.1.1 *Stellar winds with constant velocity fields (CVF)*

In this easy case, one assumes that the stellar winds reach the asymptotic velocities v_{i_∞} very quickly, and that beyond this point they expand with constant velocities. According to Pauldrach, Puls & Kudritzki (1985) this assumption may be used for the WR component of V444 Cygni, but does not hold very well for the O-star. The fields

$$v_i := v_i(r_i)=v_{i_\infty}=\text{constant}, \quad (2.32)$$

$$\rho_i := \rho_i(r_i)=\beta_i/r_i^2, \ \beta_i := A_i/4\pi v_{i_\infty}=C_i/v_{i_\infty}, \quad (2.33)$$

do not take into account the finite radii R_i of the stars. For all combinations of C_i and v_{i_∞} there exists a stagnation point $x_0 \in (-a, +a)$ between the stars. Using (2.33) and writing

$$a_i := a_i(r_i)=\Gamma_i/r_i^4, \ \Gamma_i := C_i v_{i_\infty}, \quad (2.34)$$

we note that each star is completely described by one parameter, namely Γ_i. The stagnation point follows from

$$\Gamma_1(x_0-a)^2-\Gamma_2(x_0+a)^2=0. \quad (2.35)$$

A very simple case arises for $\Gamma_1=\Gamma_2$ leading to $x_0=0$, $x(\rho)\equiv 0$ and the normal vector $(1, 0, 0)^t$, i.e. the interface is the plane $x=0$ as expected. The second case may be $\Gamma_1>\Gamma_2$, i.e. star '2' has the strong radiation field. The treatment of the case $\Gamma_2<\Gamma_1$ would be analogous. Defining

$$\Gamma := \frac{\Gamma_2+\Gamma_1}{\Gamma_1-\Gamma_2}>1, \ \gamma^2 := \Gamma_1/\Gamma_2, \ g_i := \Gamma_i^{1/2}, \quad (2.36)$$

the stagnation point takes the form

$$x_0=a[\Gamma \pm (\Gamma^2-1)], \quad (2.37)$$

i.e. for all Γ there are two real solutions corresponding to one parallel and one antiparallel velocity distribution. For the boundary interface, the antiparallel distribution is the relevant one and is related to a stagnation point $x_0 \in (0, a)$, which, or all $\Gamma>1$, is given by

$$x_0=a[\Gamma-(\Gamma^2-1)^{1/2}]=a\frac{g_1-g_2}{g_1+g_2}=a\frac{\gamma-1}{\gamma+1}. \quad (2.38)$$

If, vice versa, the stagnation point x_0 is known, the ratio $\gamma^2 := \Gamma_1/\Gamma_2$ can be calculated from

$$\gamma^2=\frac{\Gamma_1}{\Gamma_2}=\frac{A_1-v_{1_\infty}}{A_2 v_{2_\infty}}=\left(\frac{a+x_0}{a-x_0}\right)^2. \quad (2.39)$$

This relation will be used later in order to connect the trajectorial model (Kallrath 1989, 1990) and the hydrodynamical models used in this paper by identifying the stagnation points.

In case 2 the boundary interface is completely determined by the ratio of the two physical parameters Γ_1 and Γ_2. The DE now reads

$$\rho x'_{1,2} = x - a\frac{g_1 V - kg_2 U}{g_1 V + kg_2 U} = x - a\frac{\gamma^2 V - kU}{\gamma^2 V + kU}. \qquad (2.40)$$

From (2.18) we further derive the relations determining the sign of k,

$$v_{1n} = +2g_2 aV/(1+x'^2)^{1/2}k, \qquad (2.41)$$

$$v_{2n} = -2g_2 aU/(1+x'^2)^{1/2}. \qquad (2.42)$$

The condition (2.6), i.e. $v_{1n}v_{2n} < 0$, can only be fulfilled if $k = +1$. Note that with $k = +1$ the differential equation (2.40) is regular.

Differentiating (2.40) with respect to ρ we obtain the curvature

$$\rho x'' = 8a^2 g_1 g_2 (3x^2 + a^2 + 2\rho x + \rho x')/(g_2 V + g_1 U)^2 \qquad (2.43)$$

which is always positive, i.e. $x'' \geq 0$.

It is also interesting to discuss the asymptotic behaviour of the solution. For all $x \in \mathbb{R}_0^+$ we note that $U \leq V$. According to (2.20) in the limit ($x \to \infty$, $\rho \to \infty$), we have $U \approx V$ and thus approximately

$$\rho x'_{1,2} = x + x_0, \qquad (2.44)$$

leading to the asymptotic solution of differential equation (2.20)

$$x(\rho) = C\rho - x_0, \qquad (2.45)$$

where C is an integration constant. The geometrical interpretation is that we get straight lines as the asymptotic approximation to $x(\rho)$, i.e. a cone in the three-dimensional problem. The top of the cone is positioned at $-x_0$. The numerical integration for some parameters $\gamma^2 = \Gamma_1/\Gamma_2$ shows in Fig. 1 that the asymptotic behaviour starts very early, leading almost to a cone in the three-dimensional space. The difference between this family of curves and that plotted in fig. 4 in Girard & Willson (1987) is that ours are not straightened up so fast, since the centrifugal pressure of matter of the O-star flowing along the interface has not yet been taken into account in this simplified CVF approach. The boundary interface could also be approximated by a hyperboloid,

$$\left(\frac{x+x_0}{2x_0}\right)^2 - \left(\frac{\rho}{\rho_0}\right)^2 = 1, \rho \geq 0, x \geq x_0, \qquad (2.46)$$

leading to an asymptotic straight line

$$x_\infty(\rho) = \frac{2x_0}{\rho_0}\rho - x_0, \qquad (2.47)$$

and

$$\rho x' = (x + x_0)[1 + (\rho/\rho_0)^2]^{-1}. \qquad (2.48)$$

This relation approximates, in the limit $\rho \to \infty$, to the DE (2.44), i.e. the curve $x(\rho)$ and the hyperbola defined in (2.46) have the same asymptotic straight line.

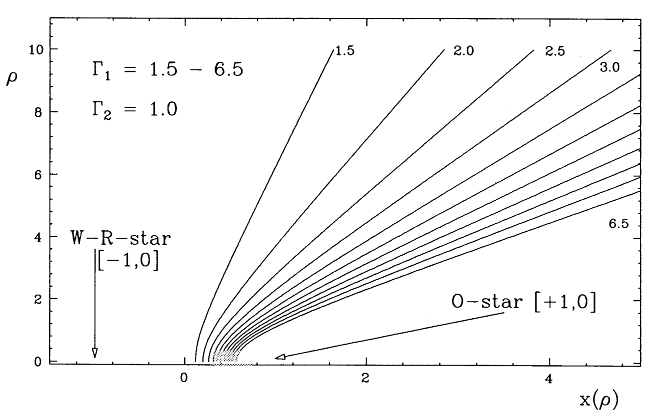

Figure 1. Pressure equilibrium surfaces in constant velocity fields derived from the Newtonian approximation. These curves are parametrized only by the ratio $\gamma^2 = \Gamma_w/\Gamma_0 = A_w/A_0$ of the mass-loss rates of both stars. In three-dimensions, they may be well approximated by cones or hyperboloids.

2.1.2 Stellar winds with quadratically decreasing acceleration (QDA)

The general solution (2.4) also allows us to choose fields like

$$\boldsymbol{v}_i := v_i(r_i) = v_{i_\infty} f(r_i, R_i)\, \boldsymbol{e}_{r-r_{xi}}, \qquad (2.49)$$

$$\rho_i := \rho_i(r_i) = \beta_i r_i^{-2}/f(r_i, R_i), f(r_i, R_i) := [1 - (R_i/r_i)^\alpha]^\beta, \qquad (2.50)$$

which are also used by Shore & Brown (1988). Note that for $R_1 = R_2 = 0$ this model reduces to that of the previous section. Thus again we use the definition (2.34) $\Gamma_i = C_i v_{i_\infty}$. α and β are empirical constants which allow us to investigate a whole class of models. The parameter β determines how fast the wind reaches its terminal velocity. From (2.50) we derive the accelerations

$$\boldsymbol{a}_i = \boldsymbol{a}_i(r_i) = \tfrac{1}{2} v_{i_\infty}^2 R_i r_i^{-2} (R_i/r_i)^{\alpha-1} f(r_i, R_i)^{2-\beta^{-2}}\, \boldsymbol{e}_{r-r_{xi}}. \qquad (2.51)$$

Castor *et al.* (1975) used $\alpha = 1$ and estimated $\beta = 1/2$. A later work by Friend & Abbott (1986) based on more detailed calculations gave $\beta \approx 0.8$, but we will use the original values since $\alpha = 1$ and $\beta = 1/2$ lead to quadratically decreasing accelerations which will be discussed below. Such a behaviour is to be expected if there is a strong radiation pressure in a field of constant opacity κ.

The model described by (2.49–2.50) considers that the stars have non-vanishing radii R_i. One disadvantage is the singularity at the surface of the stars, i.e.

$$\lim_{r_i \to R_i} \rho_i(r_i) = \infty, \lim_{r_i \to R_i} v_i(r_i) = 0, \lim_{r_i \to R_i} \boldsymbol{a}_i(r_i) = 0. \qquad (2.52)$$

The stagnation point x_0 now follows from the transcendental equation

$$\gamma^2 := \Gamma_1/\Gamma_2 = \frac{A_1 v_{1_\infty}}{A_1 v_{1_\infty}} = \left[\frac{a + x_0}{a - x_0}\right]^2 \left\{\frac{1 - [R_2/(a - x_0)]^\alpha}{[R_1/(a + x_0)]}\right\}^\beta. \qquad (2.53)$$

In some numerical tests, we investigated for $a = 1$, $R_1 = R_2$, $\alpha = 1$, $\beta = 1/2$ and $\Gamma_2 = 1$ how x_0 varies with $\Gamma_1 \geq 1$. x_0 is plotted in Fig. 2 as a function of γ^2. Beginning at $\gamma^2 = 8$, (2.53) has no root between $-a - R_1$ and $a - R_2$, i.e. within the scope of this model there is no stagnation point on the x-axis, although we note that the pressure terms have been neglected.

2.2 Extended boundary layers with mass and momentum conservation (MM)

The NA is physically based only on the conservation of the orthogonal momentum flux. This assumption is equivalent to the assumption of vanishing mass flow within the interface. In this section we use a set of ordinary differential equations describing the conservation of mass and momentum based on a general description of axisymmetric, hypersonic and hydromagnetic flow developed by Giuliani (1982). In particular, this model includes consistently a centrifugal acceleration term of matter drifting along the shell. We also refer to the modelling of CVFs by Huang & Weigert (1982) and Girard & Willson (1987).

The formalism of Giuliani is applied to the radial symmetric density and velocity fields already introduced in the previous section. Again, according to Fig. 3, the Wolf–Rayet star is star '1' and the O-star is '2', at positions $(-a, 0)$ and $(+a, 0)$. Furthermore, spherical polar coordinates (R_1, θ_1) and (R_2, θ_2) are used. The steady-state fields now appear to be

$$\rho_i v_i = A_i/4\pi R_i^2, \quad \rho_i^* := (A_i/4\pi R_i^2)/v_{i_\infty}, \quad i = 1, 2. \tag{2.54}$$

If R_i^* denote the stellar radii, and if we choose fields of the form

$$\rho_i = \rho_i^*/f_i, \quad v_i = v_{i_\infty} f_i, \ f_i := [1-(R_i^*/R_i)^\alpha]^\beta, \tag{2.55}$$

according to (2.51), we can model fields with QDAs if we use $(\alpha = 1, \ \beta = \frac{1}{2})$. All fields used to describe the interface are represented as functions of θ_1. The relation between the relevant geometrical coordinates R_1, ζ, and θ_1 is given by Giuliani (equation 5), i.e.

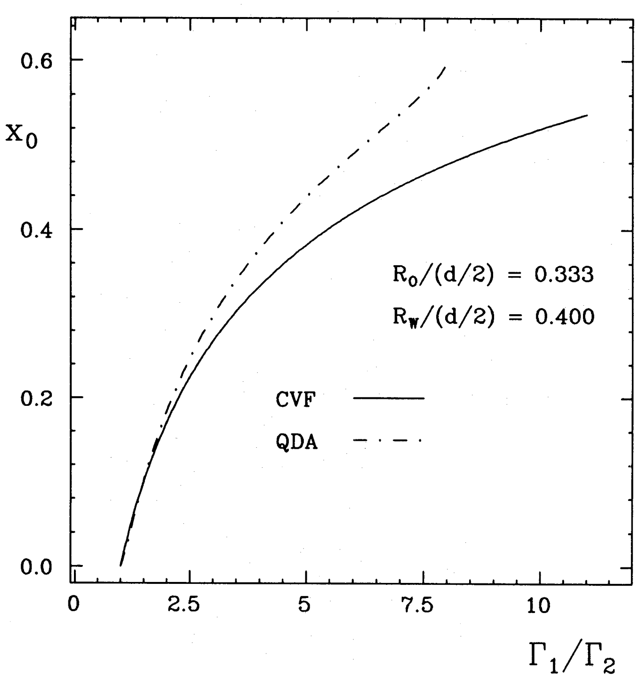

Figure 2. Stagnation-point x_0 in the CVF and QDA model as a function of $\gamma^2 = \Gamma_w/\Gamma_0 = A_w v_w / A_0 v_0$. Note that there exists a reflection point in the stagnation curve derived in the QDA. Furthermore, in the QDA there is a stagnation point only in a limited range of γ^2 while the solid line representing the stagnation point in the CVF model can be continued infinitely, approaching the constant line $x_0 = a$.

$$\tan \zeta(\theta_1) = -\frac{1}{R_1} \cdot \frac{dR_1}{d\theta_1} = -\frac{1}{R_1} \cdot R_1' = -[\ln R_1]', \tag{2.56}$$

where we use $'$ to symbolize differentiation with respect to θ_1. The equations describing the conservation of parallel and orthogonal momentum, for $\boldsymbol{u} = 0$, $\boldsymbol{B} = 0$, and shell thickness $\Delta = 0$, take the form

$$0 = -\rho_2 v_{\perp_2}(v_{\Pi_2} - v_\Pi) + \rho_1 v_{\perp_1}(v_{\Pi_1} - v_\Pi) \sigma v_\Pi \frac{\cos \zeta}{R_1} v_\Pi', \tag{2.57}$$

$$0 = -\rho_2 v_{\perp_2}^2 - p_2 + \rho_1 v_{\perp_1}^2 + p_1 + \sigma v_\Pi^2 \frac{\cos \zeta}{R_1}[1 + \zeta']. \tag{2.58}$$

For $\Delta > 0$, σ is the column density within the interface measured along the normal on to the centre line of the shell. However, for $\Delta = 0$, σ degenerates to the surface density ρ_F on the shell itself. While σ depends on θ_1 as well as on the distance to the centre-line, ρ_F depends only on θ_1. The components of the velocity follow directly from Fig. 3,

$$v_{\Pi_2} = +v_2 \sin(\Phi - \zeta), \ v_{\perp_2} = v_2 \cos(\Phi - \zeta), \ \Psi = 180 - (\theta_1 + \Phi) \tag{2.59}$$

$$v_{\Pi_1} = -v_1 \sin \zeta, \qquad v_{\perp_1} = v_1 \cos \zeta. \tag{2.60}$$

The terms in (2.57) represent the parallel momentum flux entering the interface and the resulting gradient of the momentum flux within the shell. The four first terms in (2.58) describe the kinetic pressure and thermal pressure of both wind flows. These terms are equivalent to those in equation (2.3) derived within the framework of the NA. The third term describes a centrifugal acceleration term of matter drifting along the shell.

The equation for the conservation of mass follows (Appendix A) by integration of all matter which enters the shell up to an angle of θ_1,

$$A_1[1 - \cos \theta_1] + A_2[1 + \cos(\Phi + \theta_1)] = 4\pi R_1 \sin \theta_1 \sigma v_\Pi. \tag{2.61}$$

In Cartesian coordinates $[x, \eta = (y^2 + z^2)^{1/2}]$, as in Huang & Weigert, this is equivalent to

$$\sigma v_\Pi = A_1 \frac{R_1 - (x + a)}{4\pi R_1 \eta} + A_2 \frac{R_2 - (a - x)}{4\pi R_2 \eta}. \tag{2.62}$$

For the numerical analysis it is worthwhile to introduce the dimensionless variables suggested by Girard & Willson (1987),

$$r_i = R_i/D, \ r_i^* = R_i^*/D, \ v = v_\Pi / v_{2_\infty}, \ q = \sigma v_{2_\infty} \frac{D}{A_2}, \tag{2.63}$$

and the ratios

$$m := A_1/A_2, \ w = v_{1_\infty}/v_{2_\infty}, \ \gamma^2 := mw, \ f := f_1/f_2. \tag{2.64}$$

The product mw is equal to the quantity $\gamma^2 := \Gamma_1/\Gamma_2$ used in the NA (2.36, 2.53). If the pressures p_i are neglected, we derive the following set of equations (Kallrath 1989, for $R_i^* = 0$ these equations are those used by Girard & Willson):

$$r_1' = -r_1 \tan \zeta, \Rightarrow r_1'' = -r_1 \tan \zeta - r_1(1 + \tan^2 \zeta)\, \zeta', \tag{2.65}$$

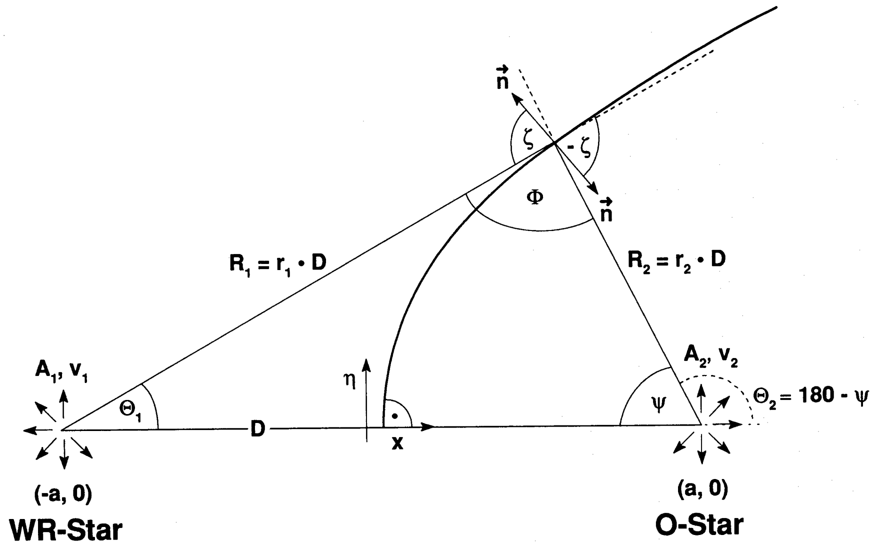

Figure 3. Schematic plot of the pressure-equilibrium surface in the binary stellar wind problem to illustrate the angles and other quantities used in the model.

$$v' = \frac{r_1}{4\pi q v \cos\zeta}\left\{\frac{-\cos(\Phi-\zeta)[f_2\sin(\Phi-\zeta)-v]}{r_2^2} + m\cos\zeta\left(\frac{-f_1 w\sin\zeta - v}{r_1^2}\right)\right\}, \tag{2.66}$$

$$\zeta' = \frac{r_1}{4\pi q v^2\cos\zeta}\left[f_2\frac{\cos^2(\Phi-\zeta)}{r_2^2} - mwf_1\frac{\cos^2\zeta}{r_1^2}\right] - 1, \tag{2.67}$$

where q, r_2^2 and Φ are also functions depending on θ_1,

$$q = [1+\cos(\Phi+\theta_1)+m(1-\cos\theta_1)]/(4\pi r_1 v\sin\theta_1), \tag{2.68}$$

$$r_2^2 = 1 + r_1^2 - 2r_1\cos\theta_1,\ r_1(0)+r_2(0)=1, \tag{2.69}$$

$$\cos\Phi = \frac{r_1^2+r_2^2-1}{2r_1r_2} = \frac{r-\cos\theta_1}{r_2},\ \sin\Phi = \frac{\sin\theta_1}{r_2} \tag{2.70}$$

following from (2.58) and from the geometry. The initial conditions for $\theta_1 = 0$ are derived from the stagnation point which follows from

$$\rho_1 v_1^2 = \rho_2 v_2^2. \tag{2.71}$$

If $R_i^* = 0$ or $f_i = 1$ then the stagnation point can be calculated analytically. In agreement with (2.38) we achieve

$$r_s := r_1(\theta_1 = 0) = \frac{\gamma}{1+\gamma},\quad x_s = a\frac{\gamma-1}{\gamma+1}. \tag{2.72}$$

Because of the singular character of (2.66–2.68) at $\theta_1 = 0$, besides

$$(r_1, v, \zeta)_0 = (r_s, 0, 0),\quad \Phi_0 = 180° \tag{2.73}$$

we need the values of the derivatives at $\theta_1 = 0$ for using the Taylor series representation of $(r_1, v, \zeta)_0'$. Using L'Hospital's rule in Appendix B we derive

$$[(r_1, v, \zeta,)', q]_0 = \left[0, \frac{2}{3}\frac{w}{w+1}(1-\gamma), -\frac{4+3\gamma}{7}, \frac{3}{16\pi}\gamma\left(\frac{w+1}{w}\right)^2\right], \tag{2.74}$$

or, when taking into account the factors $f_1(0)$ and $f_2(0)$ and the abbreviations $W := wf(0)$ and $\Gamma^2 := f(0)\,\gamma^2$, the relations

$$[(r_1, v, \zeta,)', q]_0 = \left[0, \frac{2}{3}\frac{W}{W+1}(1+\Gamma)\,f_2, -\frac{4+3\Gamma}{7}, \frac{3}{16\pi}\Gamma\left(\frac{W+1}{W}\right)^2\Big/ f_2\right]. \tag{2.75}$$

We have integrated the system (2.65–2.67) with $(A_w, A_0) = (1.4, 0.25)\times 10^{21}$ g s^{-1}, $(v_w, v_0) = (1530, 2460)$ km s^{-1}, $(R_w^*, R_0^*) = (12, 10)\,R_\odot$ and $(\alpha, \beta) = (1, \frac{1}{2})$ numerically. A_0 has been determined by using the stagnation point $x_0 = 0.3$ and equation (2.39, 2.53). Thus, when identifying those curves derived with CVFs and QDA fields, the O-star has a somewhat different mass-loss rate A_0. However, A_0 is usually not known very well. Fig. 4 shows the results of our integrations indicated as the MM model, performed both for CVF ($\gamma^2 = 3.449$, $A_0 = 0.252\times 10^{21}$ g s^{-1}) and QDA fields ($\gamma^2 = 3$, $A_0 = 0.290\times 10^{21}$ g s^{-1}), with those curves derived in the trajectorial model and from the NA. Since θ_1 has been chosen as the independent variable for the integration of the DES (2.65–2.67), the integration is limited to $(0, \theta_\infty)$, where $\tan\theta$ is just the gradient of the asymptotic straight line of the shell. For the set of parameters defined above we have a numerical value of $\theta_\infty \approx 68°$. What is remarkable is the almost perfect agreement between the envelope derived by the two-fixed-centre problem and the boundary derived in this section with the QDA ansatz. This justifies our argument to account for non-inertial effects in hydrodynamics frameworks by applying corrections derived from trajectorial models. The interface derived in this section, and the flow fields external to it, will serve as initial data for numerical simulations of the BSWP in the forthcoming paper.

In the limiting case of a binary system with an infinite semi-major axis (Kallrath 1989) and one star blowing with infinite strength, one arrives back at the model of Baranov, Krasnobaev & Kulikovski (1971) describing the interaction of the solar wind and the local interstellar medium.

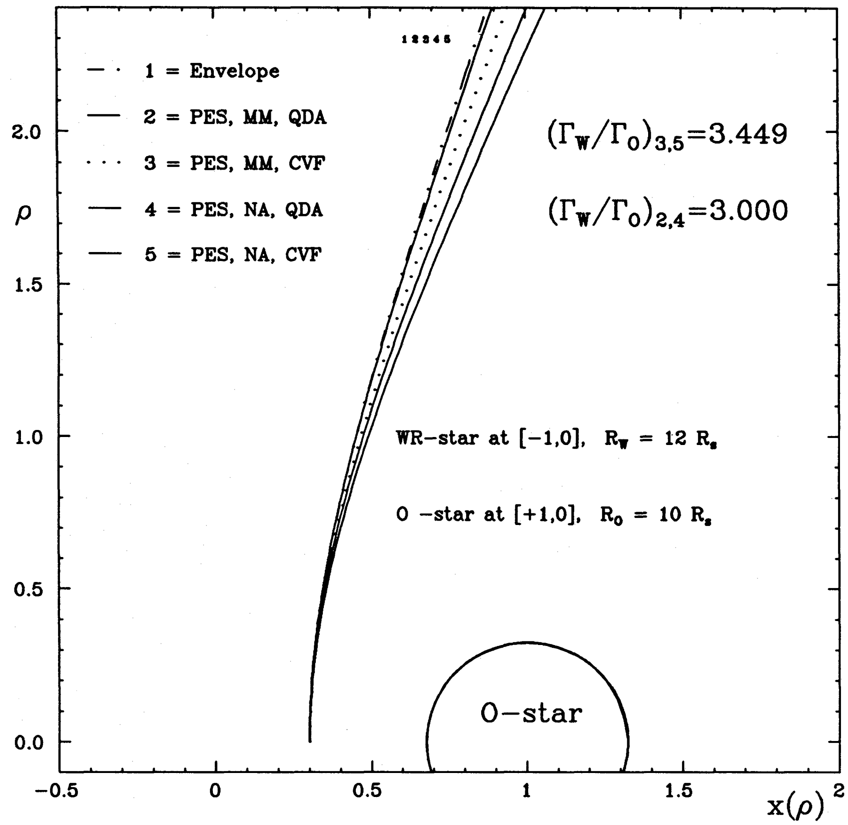

Figure 4. Pressure-equilibrium surfaces and the envelope in the two-fixed-centre-problem. Note that the pressure-equilibrium surfaces derived from the MM model supplied by QDA fields and the envelope derived from the trajectorial model (Kallrath 1989, 1990) fit best to each other. Their curvature is smaller than those of all other curves. The different values of γ^2 when using CVF and QDA fields represent somewhat different mass-loss rates of the O-star but lead to the same stagnation point x_0 which makes a comparison of both models possible.

3 COMPARISON OF THE RESULTS DERIVED FROM DIFFERENT MODELS

3.1 The envelope in the (repulsive) two-fixed-centre problem

This model can be derived from the Navier–Stokes equations by neglecting (a) all friction effects, and (b) the gradient of the thermal pressure p. Furthermore, (c) the effect of the radiation pressure is simplified to a repulsive $1/r$-potential, and finally (d) it is limited to the case of vanishing orbital velocity, i.e. to the limit $\omega \to 0$. The advantage is that this ansatz allows an analytic treatment of the problems expressing the trajectories in terms of elliptic functions, and also leading to a transcendental equation for the envelope. The gravitation itself is modelled correctly. The effect of the radiation pressure should certainly be the subject of a more rigorous theory of radiation transport, but the $1/r$ may be a first step in the right direction. Since only low-angle trajectories cross other trajectories, the assumption of vanishing thermal pressures turns out to be possible in the first step. The negligible differences between the envelope and the boundary interface derived as a pressure equilibrium surface justify the use of a trajectorial model. The trajectorial models also have the advantage that they are more flexible towards implementing more physics, e.g. the effect of resonance lines. Furthermore, they are useful in the description of dust-driven winds, or the dust expansion of inviscid dust shells.

3.2 Trajectories in the synodic system: $\omega > 0$

This model is identical to the two-fixed-centre problem with one exception: it accounts for non-vanishing orbital velocity, and thus leads to the (repulsive) restricted three-body problem. Its advantage is that it will support an estimation of the effect of non-inertial forces, which lead to a small turn of the boundary surface by an angle about 10°. Thus, it justifies the use of axisymmetric models in later analyses.

3.3 Newtonian approximation (NA)

This pressure-equilibrium ansatz is essentially based on the requirement of conservation of orthogonal momentum flow on both sides of the unknown boundary interface which is assumed to be of zero thickness. The zero thickness assumption is, as will be shown in a forthcoming paper, over-simplified. It would only be valid if there are processes available which efficiently consume the thermal energy of the shocked gas. The interface is solved by (numerical) integration of differential equations which requires furthermore the predetermination of the external flow fields, i.e. ρ_i, $\boldsymbol{v}_i$ and p_i. This method is better for external flows with high Mach number. The effect of gravitation and radiation pressure is only implicitly contained in the density and velocity fields, e.g. by using fields which lead to a quadratically decreasing acceleration.

The geometry of the integrated boundaries does not differ much from the envelope derived in a trajectorial model. Since the thermal pressure has been neglected, the curvature of the boundary curve does not change its sign. The NA describes a physical situation in which matter hits the zero thickness interface, and is instantaneously changed completely into radiation, which is radiated isotropically.

3.4 Extended boundary layers with mass and momentum conservation (MM)

The basic assumption again is the thin-shell approach. The conservation of mass and momentum is fully taken into account. The obvious difference, when compared with the results derived from the NA, is that the curvature of the boundary curve decreases much faster. This can be easily understood in terms of the centrifugal pressure of the O-star material flowing along the shell. The fact that the integration of the boundary interface based on given QDA fields agrees well with the envelope derived from the two-fixed-centre potential shows that the thermal pressure is indeed negligible. However, this picture will change drastically when shocks and a non-vanishing thickness of the interface are taken into account.

4 CONCLUSIONS

The binary stellar wind problem (BSWP) is investigated within the framework of the NA for a typical set of parameters describing a hot (WR/O) binary like HD 152270 (the stars are $60\,R_\odot$ separated from each other). The interface between both stellar wind flows is determined from the conservation of orthogonal momentum flux on both sides of the interface. Under the assumption of negligible thermal pressure, for given constant velocity fields and associated quadratically decreasing density fields, and fields with quadratically decreasing acceleration, the boundary surface, further assumed to be of zero thickness (see forthcoming paper for validity), is numerically computed by integration of an ordinary non-linear first-order differential equation.

The same pre-defined fields are used in an extended model based on a general formalism by Giuliani (1982) describing hypersonic axisymmetric flows and accounting for the conservation of mass, and parallel and orthogonal momentum, leading to a system of three ordinary, non-linear coupled differential equations. The numerical integration yields a boundary curve which might be approximated by a hyperboloid.

The results from these integrations are compared with the envelope derived within the framework of the two-fixed-centre problem by Kallrath (1989, 1990). It turns out that the envelope and the interface corresponding to given fields with quadratically decreasing acceleration fit nearly identically to each other. The results from this analysis and the flow field around the stars are used as initial data for the numerical simulations in a subsequent paper. There, the axisymmetric binary stellar wind problem is investigated in terms of the numerical integration of the hyperbolic system of equations describing the conservation of mass, momentum and energy, which govern the stellar wind fluid dynamics.

ACKNOWLEDGMENTS

The author gratefully acknowledges many encouraging discussions with H.-J. Fahr and H. Schmidt and useful comments by the referee. This work has been generously supported by the Cusanuswerk Foundation.

REFERENCES

Baranov, V. B., Krasnobaev, M. G. & Kulikovski, M. S., 1971. *Sov. Phys.-Dokl.*, **15**, 791.
Bulirsch, R. & Stoer, J., 1965. *Numerische Mathematik*, **8**, 1.
Castor, J. I., Abbott, D. C. & Klein, R. I., 1975. *Astrophys. J.*, **195**, 157.
Fahr, H. J., Ratkiewicz-Landowska, R. & Grezdzielski, S., 1986a. *Adv. Space Res.*, **6** (1), 389.
Fahr, H. J., Grezdzielski, S. & Ratkiewicz-Landowska, R., 1986b. *Ann. Geophys.*, **6** (4), 337.
Friend, D. B. & Abbott, D. C., 1986. *Astrophys. J.*, **311**, 701.
Girard, T. & Willson, I. A., 1987. *Astr. Astrophys.*, **183**, 247.
Giuliani, Jr. J. L., 1982. *Astrophys. J.*, **256**, 624.
Huang, R. Q. & Weigert, A., 1982. *Astr. Astrophys.*, **112**, 281.
Kallrath, J., 1989. *PhD thesis*, Bonn University (FRG).
Kallrath, J., 1990. *Celestial Mechanics and Dynamical Astronomy*, submitted.
Moffat, A. F. J., Lamontagne, R., Shara, M. M., McAlister, H. A., 1986. *Astr. J.*, **91**, 1392.
Neutsch, W., 1979. *Veröff. astr. Inst. Univ. Bonn*, **93**.
Neutsch, W., 1986. *Habilitation thesis*, Bonn University, unpublished.
Pauldrach, A., Puls, J. & Kudritzki, R. P., 1985. *Astr. Astrophys.*, **148**, L1.
Shore, S. N. & Brown, D. N., 1988. *Astrophys. J.*, **334**, 1021.

APPENDIX A: DERIVATION OF THE MASS CONSERVATION EQUATION

Let us consider the mass flow on the boundary surface or boundary curve at a point corresponding to θ_1. In this appendix we refer to the nomenclature set up by Giuliani (1982). The mass flow $\sigma v_\Pi(\theta_1)$ in such a point follows from the integration

$$\int_0^{\theta_1} [\text{mass flow}(\theta)_1 + \text{mass flow}(\theta)_2]\, d\theta\, d\varphi, \tag{A1}$$

i.e. only the orthogonal components of the flow fields hitting the interface are considered.

Since only time-dependent fields are considered, Giuliani's equation (32), for $\boldsymbol{u}=0$, simplifies to

$$0 = -v_{\perp_2}\rho_2 \frac{R\sin\theta}{\cos\zeta}\, d\theta\, d\varphi\,|\,R_2 + v_{\perp_1}\rho_1 \frac{R\sin\theta}{\cos\zeta}\, d\theta\, d\varphi\,|\,R_1 - \partial_\theta(v_\Pi \sigma R\sin\theta)\, d\theta\, d\varphi. \tag{A2}$$

Due to the axial symmetry, integration over $d\varphi$ yields a factor 2π on both sides of the equation. For an infinitely thin shell, we have

$$R_{|R_2} = R_2,\ R_{|R_1} = R_1,\ R_{|R} = R_1. \tag{A3}$$

Furthermore, we note the relations

$$\cos\zeta_{|R_2}=\cos(\zeta+\Phi),\ \cos\zeta_{|R_2}=\cos\zeta,\ \theta_{|R_2}=180-(\theta+\Phi),\tag{A4}$$

which transforms (A2) into the simplified expression

$$0=-v_2\rho_2R_2^2\sin[180-(\theta+\Phi)]\,d\theta + v_1\rho_1R_1^2\sin\theta\,d\theta-\partial_\theta(v_\Pi\sigma R_1\sin\theta)\,d\theta.\tag{A5}$$

Using the relation (2.7) for A_1 and A_2 and the definition $\Psi:=180-(\theta+\Phi)$ we obtain

$$0=-\frac{1}{4\pi}A_2\sin\Psi(-d\Psi) +\frac{1}{4\pi}A_1\sin\theta\,d\theta-\partial_\theta(v_\Pi\sigma R_1\sin\theta)\,d\theta.\tag{A6}$$

Integration yields

$$0=\int_{180}^{\Psi_1}A_2\sin\Psi\,d\Psi+\int_0^{\theta_1}A_1\sin\theta\,d\theta -4\pi\int_0^{\theta_1}\partial_\theta(v_\Pi\sigma R_1\sin\theta)\,d\theta.\tag{A7}$$

Furthermore, we derive

$$4\pi v_\Pi\sigma R_1\sin\theta\,|_0^{\theta_1}=-A_2\cos\Psi\,|_{180}^{\Psi_1}-A_1\cos\theta\,|_0^{\theta_1},\tag{A8}$$

$$4\pi v_\Pi\sigma R_1\sin\theta_1=A_2(1-\cos\Psi_1)+A_1(1-\cos\theta_1).\tag{A9}$$

Since
$\cos(\pi-x)=-\cos(-x)=-\cos x$, we get

$$4\pi v_\Pi\sigma R_1\sin\theta_1=A_2[1+\cos(\theta_1+\Phi)]+A_1(1-\cos\theta_1),\tag{A10}$$

which can also be expressed in Cartesian coordinates using the relations

$$\cos\theta_1=\frac{x+a}{R_1},\quad 1-\cos\theta_1=\frac{R_1-(x+a)}{R_1},\quad \sin\theta_1=\frac{\eta}{R_1}\tag{A11}$$

and

$$1-\cos\Psi=\frac{R_2-(a-x)}{R_2},\tag{A12}$$

finally leading to the expression (6) used by Huang & Weigert (1982)

$$\sigma v_\Pi=A_1\frac{R_1-(x+a)}{4\pi R_1\eta}+A_2\frac{R_2-(a-x)}{4\pi R_2\eta}.\tag{A13}$$

APPENDIX B: INITIAL VALUES FOR THE INTEGRATION

The stagnation point $r_s=r_1(\theta_1=0)$ follows as in the NA from

$$\rho_1v_1^2=\rho_2v_2^2.\tag{B1}$$

Using the density and velocity fields defined by (2.54–2.55),

$$\rho_iv_i=A_i/4\pi R_i^2,\ \rho_i^*:=\rho_iv_i/v_{i_\infty},\ \rho_i=\rho_i^*/f_i,\ v_i=v_{i_\infty}f_i,\tag{B2}$$

$$f_i:=[1-(R_i^*/R_i)^\alpha]^\beta,\tag{B3}$$

we obtain

$$r_1/(1-r_1)=(mwf)^{1/2},\ m:=A_1/A_2,\ w:=v_{1_\infty}/v_{2_\infty},\ f:=f_1/f_2.\tag{B4}$$

Only for $f_1=f_2=1$ can (B4) be solved analytically. Otherwise the root has to be determined numerically. Once r_s is found, from $\theta_1=0$ and

$$(r_1,v,\zeta)_0=(r_s,0,0),\tag{B5}$$

we can derive the derivatives by applying L'Hospital's rule. To begin with, let us discuss this problem only for $f_1=f_2=1$ and repeat (2.66–2.68):

$$v'=\frac{r_1}{4\pi qv\cos\zeta}\left\{\frac{-\cos(\Phi-\zeta)[\sin(\Phi-\zeta)-v]}{r_2^2} +m\cos\zeta\frac{-w\cdot\sin\zeta-v}{r_1^2}\right\},\tag{B6}$$

$$\zeta'=\frac{r_1}{4\pi qv^2\cos\zeta}\left[\frac{\cos^2(\Phi-\zeta)}{r_2^2}-mw\frac{\cos^2\zeta}{r_1^2}\right]-1,\tag{B7}$$

$$q=[1+\cos(\Phi+\theta_1)+m(1-\cos\theta_1)]/(4\pi r_1v\sin\theta_1).\tag{B8}$$

We will derive relations for $(v',q)_0$. Then $(\zeta)'_0$ can be found immediately using $(v',q)_0$. If QZ and QN denote the numerator and denominator of q, we note that from

$$r_2\sin\Phi=\sin\theta_1\Rightarrow r_2'\sin\Phi+r_2\cos(\Phi)\,\Phi'=\cos\theta_1\tag{B9}$$

$$\Rightarrow\Phi'(\theta_1\to0)=-\frac{1}{r_2}=-(\gamma+1),\ r_2'(0)=0,\tag{B10}$$

$$\mathrm{QZ}'=-\sin(\Phi+\theta_1)(1+\Phi')+m\sin\theta_1,\ \Phi(0)=0,\tag{B11}$$

$$\mathrm{QN}'=4\pi[r_1'v\sin\theta_1+r_1v'\sin\theta_1+r_1v\cos\theta_1],\tag{B12}$$

and finally the formal result

$$q_0=q(\theta_1=0)=q(\theta_1\to0)=\frac{\mathrm{QZ}'(\theta_1\to0)}{\mathrm{QN}'(\theta_1\to0)}=\frac{0}{0}\tag{B13}$$

will follow. Therefore, we have to inspect the second derivatives

$$\mathrm{QZ}''=-\cos(\Phi+\theta_1)(1+\Phi')^2-\sin(\Phi+\theta_1)\,\Phi''+m\cos\theta_1,\tag{B14}$$

$$\begin{aligned}\mathrm{QN}''=\ & r_1''v\sin\theta_1+r_1'v'\sin\theta_1+r_1'v'\sin\theta_1,\\ &+r_1'v'\sin\theta_1+r_1v''\sin\theta_1+r_1v'\cos\theta_1,\\ &+r_1'v\cos\theta_1+r_1v'\cos\theta_1+r_1v\sin\theta_1.\end{aligned}\tag{B15}$$

Differentiating (B9) once more

$$r_2''\sin\Phi+r_2'\cos\Phi+(r_2\cos\Phi)\,\Phi''+(r_2\cos\Phi)\,\Phi'=-\sin\theta_1\tag{B16}$$

and using the implication (2.69) r_1'' bounded $\Rightarrow r_2''$ bounded], we conclude that Φ'' is also bounded. Since

$\sin(\Phi+\theta_1)=0$, those terms containing higher derivatives drop out and we eventually get

$$QZ''(\theta_1\to 0)=(1+\Phi')^2+m=\gamma^2+m=\gamma^2\left(1+\frac{1}{w}\right)=\gamma^2\,\frac{w+1}{w}, \tag{B17}$$

$$QN''(\theta_1\to 0)=8\pi[r_1(0)\,v_0']=8\pi\,\frac{\gamma}{\gamma+1}\,v_0', \tag{B18}$$

and finally with

$$q_0=q(\theta_1=0)=q(\theta_1\to 0)=\frac{QZ''(\theta_1\to 0)}{QN''(\theta_1\to 0)}, \tag{B19}$$

the result

$$4\pi q_0 v_0'=4\pi q(\theta_1\to 0)\,v'(\theta_1\to 0)=\frac{1}{2}\,\gamma\,\frac{w+1}{w}. \tag{B20}$$

In order to derive another independent relation we note that

$$\cos\zeta(0)=-\cos(\Phi-\zeta)=1 \tag{B21}$$

and use the Taylor series expansion at $\theta_1=0$ for small angles θ_1,

$$v\doteq v_0'\sin\theta_1\doteq v_0'\theta_1,\ \zeta\doteq\zeta_0'\sin\theta_1\doteq\zeta_0'\theta_1. \tag{B22}$$

We substitute (B21) and later

$$r_2^{-2}=(\gamma+1)^2,\ r_1^{-2}=(\gamma+1)^2/\gamma^2 \tag{B23}$$

into (B6) leading to the right-hand side of (B6)

$$\frac{\sin(\Phi-\zeta)-v}{r_2^2}+m\left[\frac{-(w\sin\zeta)-v}{r_1^2}\right]=\frac{\sin(\Phi-\zeta)}{r_2^2}$$
$$-\gamma^2\,\frac{\sin\zeta}{r_1^2}-\left(\frac{1}{r_2^2}+\frac{m}{r_1^2}\right)v'. \tag{B24}$$

Using (B9) and

$$\sin(\Phi-\zeta)-\sin\zeta=\sin\Phi\cos\zeta-\sin\zeta\cos\Phi-\sin\zeta$$
$$=(\gamma+1)\sin\theta_1\cos\zeta-\sin\zeta(1+\cos\Phi) \tag{B25}$$

and

$$1+\cos\Phi=1-\sqrt{1-\sin^2\Phi}\doteq 1-[1-\tfrac{1}{2}\sin^2\Phi]=+\tfrac{1}{2}\sin^2\Phi$$
$$\doteq +\tfrac{1}{2}(\gamma+1)^2\sin^2\theta_1, \tag{B26}$$

we obtain

$$\sin(\Phi-\zeta)-\sin\zeta=(\gamma+1)\sin\theta_1-O(\theta_1^3)\doteq(\gamma+1)\,\theta_1-O(\theta_1^3) \tag{B27}$$

and substituting (B27) in (B24) we get eventually

$$v'^2=\frac{r_1}{4\pi q}\left[(\gamma+1)^2(\gamma+1)-\frac{w+1}{w}\,v'\right] \tag{B28}$$

or

$$4\pi q_0 v'^2=\gamma(\gamma+1)\left[(\gamma+1)-\frac{w+1}{w}\right]. \tag{B29}$$

Thus, substitution of (B20) into (B29) gives a linear equation in v', from which we easily derive

$$(v',q)_0=\left[\frac{2}{3}\,\frac{w}{w+1}\,(1+\gamma),\ \frac{3}{16\pi}\,\gamma\left(\frac{w+1}{w}\right)^2\right]. \tag{B30}$$

ζ_0' is derived similarly, but in the denominator of (B7) we make explicit use of (B22). The right-hand side of (B7) leads to

$$\frac{1}{\cos\zeta}[\cos^2(\varphi-\zeta)\,r_2^{-2}-mw\cos^2(\zeta)\,r_1^{-2}] \tag{B31}$$

$$=\frac{(\gamma+1)^2}{\cos\zeta}[(\cos\Phi\cos\zeta+\sin\Phi\sin\zeta)^2-\cos^2\zeta]$$

$$=\frac{(\gamma+1)^2}{\cos\zeta}[\cos^2\Phi\cos^2\zeta+\sin^2\Phi\sin^2\zeta$$
$$+2\cos\Phi\cos\zeta\sin\Phi\sin\zeta-\cos^2\zeta]$$

$$=(\gamma+1)^2\left[(\cos^2\Phi-1)\cos\zeta+\frac{\sin^2\Phi\sin^2\zeta}{\cos\zeta}\right.$$
$$\left.+2\cos\Phi\sin\Phi\sin\zeta\right].$$

(B6) and (B21–B23) are inserted into (B31) resulting in

$$(\gamma+1)^2\left(-\sin^2\Phi\cos\zeta+\frac{\sin^2\theta_1\sin^2\zeta}{r_2^2\cos\zeta}+2\cos\Phi\,\frac{\sin\theta_1}{r_2}\sin\zeta\right)$$

$$=(\gamma+1)^2\left[-(\gamma+1)^2\sin^2\theta_1+r_2^{-2}(\sin^2\theta_1)\,\zeta'^2\theta_1^2\right.$$
$$\left.-2^{-2}\,\frac{\sin\theta_1}{r_2}\,\zeta_0'\theta_1\right]$$

$$=(\gamma+1)^2[-(\gamma+1)^2\sin^2\theta_1+O(\theta_1^{-4})$$
$$-2(\gamma+1)(\sin\theta_1)\,\zeta_0'\theta_1]. \tag{B32}$$

Using $4\pi q v_0'^2=\frac{1}{3}\gamma(\gamma+1)$ and $r_1(\gamma+1)^2/4\pi q v_0'^2=\dfrac{3}{\gamma+1}$ from (B7) we derive

$$\zeta_0'=-3[(\gamma+1)+2\zeta_0']-1,\ \text{so}\ \zeta_0'=-\frac{4+3\gamma}{7}. \tag{B33}$$

Thus, if we summarize,

$$[(r_1,\,u\,\zeta)',q]_0=\left\{0,\frac{2}{3}\,\frac{w}{w+1}\,(1+\gamma)\,f_2,\right.$$
$$\left.-\frac{4+3\gamma}{7},\ \frac{3}{16\pi}\,\gamma\left[\frac{w+1}{w}\right]^2\Big/ f_2\right\}. \tag{B34}$$

Now, we could include the factors f_1 and f_2 and procede as above but it seems to be worth having a closer look at the differential equation system (2.65–2.68)

$$v' = \frac{r_1}{4\pi q v \cos\zeta}\left\{\frac{-\cos(\Phi-\zeta)[f_2\sin(\Phi-\zeta)-v]}{r_2^2} + m\cos\zeta\left(\frac{-f_1 w\sin\zeta - v}{r_1^2}\right)\right\},$$

$$\zeta' = \frac{r_1}{4\pi q v^2\cos\zeta}\left[f_2\frac{\cos^2(\Phi-\zeta)}{r_2^2} - mwf_1\frac{\cos^2\zeta}{r_1^2}\right] - 1. \qquad \text{(B35, B36)}$$

$$q = [1+\cos(\Phi+\theta_1)+m(1-\cos\theta_1)]/(4\pi r_1 v\sin\theta_1). \qquad \text{(B37)}$$

If one divides by f_2, one notices that in the stagnation point, since the velocity $v=0$ vanishes, then with $v \to v/f_2$, $q \to qf_2$ the relations

$$v_0'(w, f_1, f_2)/f_2 = v_0'(wf, f_1=1, f_2=1) \qquad \text{(B38)}$$

$$\zeta_0'(w, f_1, f_2) = \zeta_0'(wf, f_1=1, f_2=1) \qquad \text{(B39)}$$

$$q_0(w, f_1, f_2)\cdot f_2 = q_0(wf, f_1=1, f_2=1) \qquad \text{(B40)}$$

are valid. With $W := wf$ and $\Gamma := \gamma f^{1/2}$, we derive the initial conditions

$$[(r_1, v, \zeta,)', q]_0 = \left[0, \frac{2}{3}\frac{W}{W+1}(1+\Gamma)\, f_2, -\frac{4+3\Gamma}{7}, \frac{3}{16\pi}\Gamma\left(\frac{W+1}{W}\right)^2 \Big/ f_2\right]. \qquad \text{(B41)}$$